Multi-Vector Power Island Operation Utilizing Demand Side Response Based on a Cloud-based Optimization Strategy (CbOS)

ANGELOS PATSIDIS[1,2], (Student Member, IEEE), ADAM DYSKO[1], (Member, IEEE), CAMPBELL BOOTH[1], (Senior Member, IEEE), and DIMITRIOS TZELEPIS[1,2], (Member, IEEE)
[1]Department of Electronic and Electrical Engineering, University of Strathclyde, Glasgow, UK, G1 1XQ. (e-mail: angelos.patsidis@strath.ac.uk)
[2]Smart Power Networks Ltd., 65 More Close, London W14 9BN, UK

Corresponding author: Angelos Patsidis (e-mail: angelos.patsidis@strath.ac.uk).

ABSTRACT Intentional islanding is one of the potential strategies to mitigate risks related to total blackouts by partitioning the network into multiple power islands. This paper focuses on developing a cloud-based strategy for managing the post-islanding power islands operation considering the coupling of the electrified heating vector. At the core, a novel multi-vector cloud-based optimization strategy (CbOS) is utilized to harness the hidden flexibility of heating, ventilation and air-conditioning (HVAC) systems, resulting in reduced load shedding required to balance the power island and decreased operational costs. To maintain the sustainability of the power island, CbOS is further integrated with an additional objective of optimizing a voltage stability index and costs. The architecture upon which CbOS is built, provides the means to deploy the required software tools and its operation is tested in a generalizable power island under representative cases studies with respect to the level of controllability that CbOS is expected to have among the fleet of energy assets. The results reveal that when all energy assets are operated under CbOS, a substantial cost reduction up to 55.6% can be achieved by utilizing the flexibility stemming from the HVAC systems. Concurrently, voltage stability profiles are improved for the lines under stress.

INDEX TERMS Cloud-based optimization, demand side response, electrified heating, intentional islanding, multi-vector power island

NOMENCLATURE

Parameters

Δt	Time interval.
η_c	Charging efficiency of battery storage.
η_d	Discharging efficiency of battery storage.
B_{bp}	Susceptance of line connecting buses b and p.
C	Equivalent heat capacity.
$Cost_{SG}$	Operational cost of synchronous generator.
G_{bp}	Conductance of line connecting buses b and p.
H	Equivalent heat rate.
Q_r	Reactive power at the receiving end of line.
R_{TH}	Equivalent thermal resistance.
$T_{bld,min}$	Minimum acceptable building temperature.
$T_{bld,max}$	Maximum acceptable building temperature.
V_s	Bus voltage at sending end of line.
$VOLL$	Value of Lost Load.
$VOVS$	Value of Voltage Stability.
X	Reactance of line.
Z	Impedance of line.

Sets

$ESTO_{max}$	Energy capacity of battery storage.
N_{br}	Total number of line branches.
N_{bus}	Total number of buses.
$N_{bus_{BESS}}$	Total number of buses with a battery storage.

IEEE *Access*

Patsidis *et al.*: Multi-Vector Power Island Operation Utilizing Demand Side Response Based on a Cloud-based Optimization Strategy (CbOS)

$N_{bus_{HVAC}}$	Total number of buses with a heating, ventilation and air-conditioning (HVAC) system.
$N_{bus_{LD}}$	Total number of buses with a load.
$N_{bus_{PV}}$	Total number of buses with a solar PV.
$N_{bus_{sen}}$	Total number of sending ends of buses.
$N_{bus_{SG}}$	Total number of buses with a synchronous generator.
$N_{bus_{WT}}$	Total number of buses with a wind turbine.
$N_{line_{rec}}$	Total number of receiving ends of lines.
$T_{ambient}(b,t)$	Ambient temperature at bus b at time t.
$P_{LD}(b,t)$	Active load at bus b at time t.
$P_{PV,max}$	Maximum active power generation of solar PV.
$P_{SG,min}$	Minimum active power generation of synchronous generator.
$P_{SG,max}$	Maximum active power generation of synchronous generator.
$P_{WT,max}$	Maximum active power generation of wind turbine.
S_{BESS}	Power capacity of battery storage.
S_{HVAC}	Rated power of HVAC.
S_{max}^i	Capacity of line i.
$Q_{LD}(b,t)$	Reactive load at bus b at time t.
$Q_{PV,max}$	Maximum reactive power generation of solar PV.
$Q_{SG,min}$	Minimum reactive power generation of synchronous generator.
$Q_{SG,max}$	Maximum reactive power generation of synchronous generator.
$Q_{WT,max}$	Maximum reactive power generation of wind turbine.
V_{max}	Maximum acceptable bus voltage.
V_{min}	Minimum acceptable bus voltage.

Variables

$\delta_{bp}(t)$	Voltage angle difference between buses b and p at time t.
$P(b,t)$	Active power generation at bus b at time t.
$P^{ex}(b,t)$	Active power exchange between bus b and all interconnected buses at time t.
$K_{HVAC}(b,t)$	Power regulation % of HVAC system at bus b at time t.
$P_{Loadshed}(b,t)$	Loss of active load at bus b at time t.
$P_{PV}(b,t)$	Active power generation of solar PV at bus b at time t.
$P_{SG}(b,t)$	Active power generation of synchronous generator at bus b at time t.
$P_{WT}(b,t)$	Active power generation of wind turbine at bus b at time t.
$Q(b,t)$	Reactive power generation at bus b at time t.
$Q^{ex}(b,t)$	Reactive power exchange between bus b and all interconnected buses at time t.
$Q_{Loadshed}(b,t)$	Loss of reactive load at bus b at time t.
$Q_{PV}(b,t)$	Reactive power generation of solar PV at bus b at time t.
$Q_{SG}(b,t)$	Reactive power generation of synchronous generator at bus b at time t.
$Q_{WT}(b,t)$	Reactive power generation of wind turbine at bus b at time t.
$S(i,t)$	Power flow through line i at time t.
$S_{BESS}^c(b,t)$	Charging power of battery storage at bus b at time t.
$S_{BESS}^d(b,t)$	Discharging power of battery storage at bus b at time t.
$SoC(b,t)$	State of charge of battery storage at bus b at time t.
$T_{bld}(b,t)$	Building temperature with HVAC system at bus b at time t.
$V(b,t)$	Voltage at bus b at time t.

I. INTRODUCTION

POWER grids are experiencing a significant transition, with wide penetration of renewable resources, energy storage systems and controllable demand, dispersed among various voltage levels. The existing grid continues to serve as the backbone of this development, thus, requiring significant reinforcement in order to successfully incorporate these technologies whilst serving the ever increasing demand. Enhancements range from capital-intensive grid infrastructure upgrades to smart tailored management, automation and control applications, assisted by the advanced computation, communication and networking capabilities being offered nowadays [1], [2]. The significant penetration of renewable energy resources and the ambitious carbon targets set out within the next decades, the electrification of heating and transportation, increased integration of power electronic-based devices and decommissioning of large synchronous plants has increased the uncertainty around network stability and security of supply. Power systems are subjected to dynamic variations in their state, which under specific circumstances can lead to cascading outages and precipitate a partial or total blackout [3].

Intentional islanding serves as a potential measure to mitigate the risk stemming from cascading outages. Adoption of intentional islanding secures the system integrity downstream of the incepted network contingency while serving the local load with minimum load shedding. Intentional islanding can be classified as scheduled and unscheduled, with the former being deployed at a pre-defined time due to e.g. forecasted extreme weather conditions that could lead to network contingencies and the latter being decided following a flag from a real-time monitoring system with respect to a network abnormality [4]. Successful deployment of an intentional islanding

Patsidis *et al.*: Multi-Vector Power Island Operation Utilizing Demand Side Response Based on a Cloud-based Optimization Strategy (CbOS)

IEEE Access·

scheme pertains to solving a trilateral problem which can be disaggregated into the following [4]–[7]:

- Establish appropriate timing to initiate an intentional islanding scheme.
- Identify optimal partition of the power network by establishing the lines to be disconnected.
- Specify control actions necessary to maintain sustainability of the power island(s).

This paper primarily focuses on the last point and proposes a novel architecture to operate the power island(s) following network partitioning. Following intentional islanding, each power island must be sustainable while awaiting a reconnection command from the system operator [6]. With respect to this issue, a low volume of research has been conducted on the control actions within the formed power islands, with the literature assuming local load shedding as the predominant control to maintain the sustainability of each island [8]. The latter point presented above (i.e. control actions necessary to maintain sustainability of the power island(s)), consists of a mix of high- and low-level control actions, which maintain healthy power islands in a short- or long-term basis, achieving a dual objective: 1) supply local load in an uninterrupted manner and minimize load shedding, and 2) guarantee power is within acceptable frequency and voltage limits. Following system partitioning, each power island must be sustainable for a finite time interval while awaiting a reconnection command from the system operator [6]. With respect to this issue, a low volume of research has been conducted on the control actions within the formed power islands, with the literature assuming local load shedding as the predominant control to maintain the sustainability of the islands [8]. Other research papers investigate the optimal installation of renewable mobile power stations (RMPSs) [9], low-level control of battery systems in islanded microgrids [10] and static converter control for frequency and voltage regulation [11]. The authors in [12] have proposed a formulation which considers the low-level control in both grid-connected and islanded operation. Those papers, albeit addressing significant issues with respect to the islanded operation of an intentional power island, do not provide an end-to-end approach from the operator's perspective, lack consideration of the significantly dynamic nature of the problem, do not exploit flexibility sources to minimize load shedding and do not explore the benefits of coupled energy vectors in a multi-vector network.

The current state of the art, albeit addressing significant issues with respect to the islanded operation of an intentional power island, does not provide an approach from the operator's perspective, lacks consideration of the significantly dynamic nature of the problem, disregards the stability issues that can emerge within the power islands, does not exploit flexibility sources to minimize load shedding and does not explore the benefits of coupled energy vectors in a multi-vector network, considering especially the rapid electrification of heating. The vast majority of research surrounding intentional islanding pertains to the optimal network partition,

i.e. which lines shall be disconnected in order to create the power islands. Several research papers have tried to tackle this problem [4], [7], [13], [14], utilizing numerous methods to achieve the desired objectives while adhering to network constraints. To tackle the aforementioned gaps within the literature, this paper formulates a flexible optimization strategy and integrates it within an operational framework. This approach takes into consideration the coupled multi-vector flexibility, proposes a flexible and scalable architecture and optimizes the power island operation both in terms of cost and stability.

One of the most significant elements in today's commercial buildings and industrial units is the heating, ventilation and air-conditioning (HVAC) system, which regulates the flow and temperature of air flowing from and to a building, thus modulating the temperature and humidity. These parameters influence the comfort level of the inhabitants. HVAC systems utilize a significant portion of energy, accounting on average for 44% of total energy consumption in commercial buildings [15]. HVAC systems have been proven to provide considerable advantages towards realising net-zero carbon targets. These devices are already gaining popularity and are perceived as appropriate replacement of conventional heating systems, with incentives being proposed in many countries. Studies have been conducted in order to minimize HVAC systems energy consumption and maximize their efficiency, however HVAC systems operation is typically optimized on a single-unit and/or single-building framework thus neglecting the hidden flexibility stemming from HVAC systems within a wider multi-asset network [16] [17]. Another study, where HVAC systems were part of the optimization variables, did not consider the financial and technical incentives accompanying the optimal operation of the HVAC system [18]. The authors in [15] introduced a multi-HVAC optimization in multiple buildings under a time-of-use (ToU) tariff framework. The problem formulation considered temperature comfort levels and power feeder losses, with the aim of minimizing total energy costs, however the study did not considered control of other energy assets and emergency conditions.

To harness the flexibility of HVAC, a demand side response (DSR) mechanism is required. Demand side response manually or automatically regulates the demand in order to maintain the balance between generation and load. DSR has been identified as a solution to increase operational flexibility, provide multi-objective ancillary services from the end-user side and ultimately minimize the need for large capital expenditures associated with network reinforcements. DSR schemes, at the present, can be categorised into two main classes: price-based and incentive-based. In price-based DSR, the consumers receive market signals and respond accordingly, with the pre-defined time-of-use (ToU) tariffs being the predominant price-based DSR schemes in the electricity markets nowadays. In incentive-based DSR, consumers enter a contractual obligation with the utility to disconnect or completely reduce a part or all their demand when required [19]. DSR is deployed either by the end-user who possesses

the ultimate control over the energy asset [20] or by direct load control (DLC) DSR schemes. In DLC, demand is directly controlled and regulated by external entities which have procured the DSR scheme, meaning that these parties can directly regulate and control the end-user energy asset in a continuous manner without intervention by the end user or the autonomous controller of the energy asset [20]. The majority of the early-stage DSR schemes are mainly employed to provide peak load shaving, however, it has been argued that harnessed flexibility from demand side response has the ability to tender highly remunerative contracts for residential and industrial end users in order to participate in other than peak shaving formats of DSR schemes [21]. Large-scale deployment of DSR schemes is subject to market incentives, asset flexibility and two-way communications infrastructure between energy management systems and flexible demand. The proposed post-islanding management scheme presented in this paper assumes direct controllability over the DSR energy assets, thus DLC is utilized as the control strategy.

The key to apply a DLC scheme to support intentional islanding lies upon the utilization of measuring equipment, networking infrastructure, communication channels and network management systems. In that context, cloud computing services have manifested their pivotal role in fast, reliable, flexible and scalable software architectures, which can play a significant role towards alleviating the increased need for computing resources associated with the evolution of energy systems. Cloud computing is at the core of multiple applications in various sectors, such as finance, telecommunication, data analytics, etc. The business case and economies-of-scale derived by cloud services present an opportunity to other sectors, such as the energy sector, to adopt cloud-based solutions into their software developments. Thus far, the main cloud computing solutions used by the energy sector encompass large data storage and network monitoring [22]. Lately, a new type of cloud service has emerged, entitled Containers-as-a-Service (CaaS), manifesting itself as a highly robust cloud service capable of supporting data process with high availability, short response time, low latency and competitive costing [23]. Containers are lightweight, stand-alone virtualization instances consisting of applications and dependencies. In CaaS, end-users are able to deploy and handle proprietary applications whilst providing exceptional scalability and flexibility, consuming less computational resources and time, resulting into a considerable increase in applications of cloud solutions both at a development and deployment stage. Toolkits such as Docker provide the means to deliver packaged applications [24]. As power systems evolve, technologies such as cloud computing are becoming appealing as means of decentralising tasks and applications to the cloud [25]. The inherent decentralized nature of distributed generation requires computational intelligence that is capable to orchestrate the operation of multiple assets at the network edge. Cloud computing can shift this need towards the cloud while requiring minimum intelligence at the network edges, where energy assets are connected.

In a recent study, the authors of [26] explored the application of a cloud-edge scheme for the provision of fast flexibility services. In that paper, the optimization and forecasting are implemented on the cloud with the fast control actions occurring at the network edge, near the energy assets. The framework developed creates a set of operational scenarios for storage assets to be able to provide flexibility services. The authors introduce convex relaxations to solve the power flow problem by utilizing a second-order cone programming on a single phase network. A further study conducted in [27] also utilized a cloud-edge strategy to provide demand response using deep reinforcement learning, where cloud computing services are used for the deep learning activities, while the authors in [28] demonstrate a virtual power plant (VPP) energy trading platform deployment on the cloud. The authors of [29] propose a cloud-based scheme for control and optimization during contingencies, with the participation of demand side response, while presenting a comprehensive list of research-based demand response formulations in optimization problems. The solution comprises an IoT-based cloud platform with multiple cloud nodes in charge of the various tasks, including a DC power flow.

This paper takes these initial concepts one step forward, providing detailed mathematical formulation through an AC optimal power flow (AC OPF), thus capturing voltage, frequency and voltage angle variations which are necessary to provide accurate power dispatch schedule, introduces a flexible cloud-edge architecture and explores the coupling among the electricity and electrified heating vectors. Furthermore, it benchmarks different objective functions, subject to network particularities that would otherwise not be captured by simplified formulations (e.g. DC OPF, second-order cone programming).

Additionally, to mitigate and address any potential stability issues, various voltage stability indices were investigated as part of this research, in order to be modelled and integrated as objectives within the AC OPF [30]–[33]. Among them, the Fast Voltage Stability Index (FVSI) was chosen as an appropriate metric, as it can accurately predict voltage collapse and does not pose a significant computational burden for the overall problem formulation.

Within this paper we propose, validate and benchmark a cloud-hosted optimization-based power island management system. At the core of the system lies a multi-vector cloud-based optimization strategy (CbOS) equipped with an AC OPF with integrated demand side response by HVAC units. We focus on demonstrating the capabilities, advantages and flexibility offered by a flexible optimization-based system, which does not require high capital expenditures in physical equipment, utilizing the cloud as a basis for its operation and low-level hardware on the edge (e.g. single-board computer) for the implementation of the high-level actions. A schematic representation of the system architecture is presented in Fig. 1. The proposed cloud framework adopts the Docker containerisation technology to deploy the necessary applications in an economic, reliable and scalable manner.
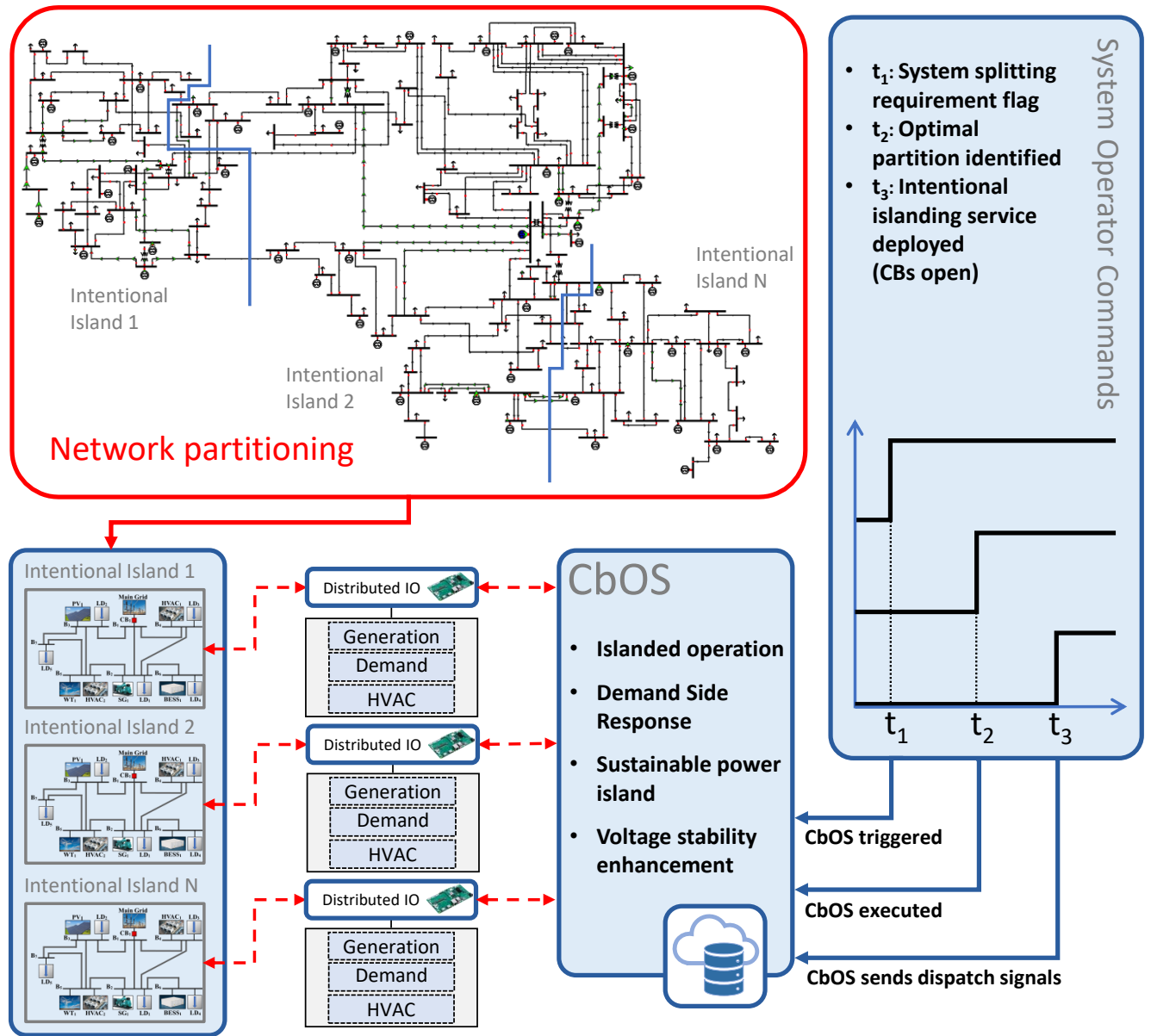
Patsidis *et al.*: Multi-Vector Power Island Operation Utilizing Demand Side Response Based on a Cloud-based Optimization Strategy (CbOS)

IEEE *Access*

FIGURE 1. CbOS-based intentional islanding operation.

Orchestration of islanded operation following intentional islanding has been identified as a contingency network service with deployment characteristics that render a cloud-based solution economical, scalable, flexible and cybersecure. Power island management via cloud computing services provides 1) no additional hardware allocation from the network operator, i.e. no up-front capital expenditure, requirement for hardware upgrades and maintenance, 2) reduced costs (work hours) with respect to IT/software updates, 3) dynamic resource allocation with respect to the computational requirements, 4) flexible, interoperable, plug-and-play architecture with the capability to migrate the solution among different providers and network operators, 5) geo-replication and failover capability for disaster mitigation, 6) cybersecure computing services, and 7) operator can choose to store the cloud products in data centers far from the network under supervision, thus guaranteeing that a local power system contingency would not disable the computing resources.

The paper is organized as follows: Section II examines the architecture and considerations for the cloud-based optimization strategy. Furthermore, it presents the mathematical representation of the AC OPF algorithm for optimally controlling the energy assets under consideration towards a flexible HVAC-oriented DSR strategy. Section III describes the case studies conducted to validate the proposed solution, demonstrates the consequent simulation results and discusses the benefits stemming from the adoption of the scheme. Finally, conclusions are drawn in Section IV.

IEEE *Access*

Patsidis *et al.*: Multi-Vector Power Island Operation Utilizing Demand Side Response Based on a Cloud-based Optimization Strategy (CbOS)

II. DEVELOPED CLOUD-BASED OPTIMIZATION STRATEGY FOR POST-ISLANDING OPERATION

Intentional islanding is contingency service which serves as a last resort measure to mitigate the risk of cascading outages that could potentially lead to a partial or total blackout. Successful deployment of an intentional islanding scheme pertains solving a trilateral problem which can be disaggregated into the following sub-problems [4]–[7]:

- Establish the appropriate timing to initiate an intentional islanding scheme.
- Identify the optimal partition of the power network by establishing the lines to be disconnected.
- Specify the control actions necessary to maintain sustainability of the power island(s).

The latter consists of a mix of high- and low-level control actions, which maintain healthy power islands in a short or long-term basis, achieving a dual objective: 1) supply local load in an uninterrupted manner and minimise load shedding, and 2) guarantee power is within acceptable frequency and voltage limits.

The main control actions over renewable generators and additional energy assets such as synchronous generation and storage is the active and reactive power dispatch signals, subject to the natural resource available, state of the generator and operational constraints. The problem of identifying the control signals over a finite number of generators within a power island can be translated into an optimization problem, where the objective function is not based upon purely economic factors but also considers the stability of the power island.

Typically, renewable generation such as solar and wind is configured to operate in a maximum power point tracking (MPPT) mode, meaning that all the available power is exported through their point of connection. However, as power networks, especially on the distribution level, integrate additional renewable resources, controllability over a proportion of the total fleet is essential to guarantee the security of supply.

Optimization in power systems is typically manifested through market clearing (day-ahead, intra-day, etc.) and the optimization for local energy communities and microgrids. However, these applications traditionally occur within the context of a centralized management system (e.g. wholesale market mechanism, microgrid controller, etc.) with pre-defined topological and operational elements. However, with power generation and demand increasing at the lower levels of the power system (i.e. distribution system), optimizing the operation at these levels is becoming a necessity.

At the core of the proposition of this paper, an AC OPF has been developed, incorporating multiple DG assets (wind, solar PV, synchronous generator, battery storage, etc.), as well as considering both fixed and flexible demand. The AC OPF is further equipped with capabilities to optimize HVAC systems, with respect to their technical particularities. Scope of the AC OPF is to optimize the operation of the network, both in terms of cost and stability, while harnessing DSR flexibility from both traditional demand and HVAC systems.

In order to benchmark the continuous supply of a satisfactory energy service, the HVAC end-user is assumed to have declared statutory limits with respect to their comfort (i.e. minimum acceptable temperature within premises assuming variable operation of HVAC). CbOS, other than control over generating units in scenarios where this is explicitly stated, has controllability over end-user equipment in two ways, namely 1) DLC over HVAC load, and 2) DLC over demand (either regulating controllable demand or load shedding).

Between operational time intervals, the optimization engine is idle, requiring no computing power. Orchestration of islanded operation following intentional islanding has been identified as a contingency network service with deployment characteristics that render a cloud-based solution economical, scalable, flexible and cybersecure. Power island management via cloud computing services provides 1) no hardware allocation from the network operator, i.e. no up-front capital expenditure, requirement for hardware upgrades and maintenance, 2) reduced costs (work hours) with respect to IT/software updates, 3) dynamic resource allocation with respect to the computational requirements, 4) flexible, interoperable, plug-and-play architecture with the capability to migrate the solution among different providers and network operators, 5) geo-replication and failover capability for disaster mitigation, 6) cybersecure computing services, and 7) operator can choose to store the cloud products in data centers far from the network under supervision, thus guaranteeing that a local power system contingency would not disable the computing resources.

The case studies conducted and presented in Section III focus on the provision of power schedules utilizing hidden flexibility from HVAC systems. This work demonstrates the added value and decreased load shedding required from utilizing DSR from HVAC systems to ensure secure and reliable operation of the power island while examining the technical and financial impact of optimizing both cost and voltage stability.

The contributions of this paper are summarized hereafter:

- A novel cloud-based optimization strategy (CbOS) capable of operating a power island.
- A novel multi-vector AC OPF incorporating a HVAC-based DSR scheme and a voltage stability metric to ensure power island sustainability.
- Proposition of a low-cost, flexible and scalable digital architecture for adoption by network operators.
- Benchmarking of DSR from HVAC systems under various comfort level limits.
- Validation of various objective functions, eventually accounting for both cost and voltage stability in a single formula.

A. MULTI-VECTOR CLOUD-BASED OPTIMIZATION SCHEME (CBOS) ARCHITECTURE

This research proposes a hybrid cloud-edge strategy with the following tasks split between the cloud and the edge intelli-

Patsidis *et al.*: Multi-Vector Power Island Operation Utilizing Demand Side Response Based on a Cloud-based Optimization Strategy (CbOS)

IEEE *Access*

gence: 1) Cloud containers are in charge of forecasting natural resources such as solar irradiance, temperature and wind speed, and demand. An additional cloud container is in charge of solving the AC OPF problem and sending the necessary datasets to the edge devices. 2) The edge devices require minimal computational capabilities and storage. These devices act primarily as interfaces among the cloud and the energy assets, utilizing communication protocols (e.g. TCP/IP) to operate the energy assets. In case of communication failure, the edge device identifies the lack of communication upstream (cloud) and utilizes the setpoints from the latest power schedule for the next interval(s) which although outdated shall be available to be used. In that case, the cloud platform identifies the failure and caters accordingly by assuming the utilization of the outdated setpoint(s) by the asset(s). The architecture described above, comprising the cloud, edge and asset layers, is presented in Fig. 2.
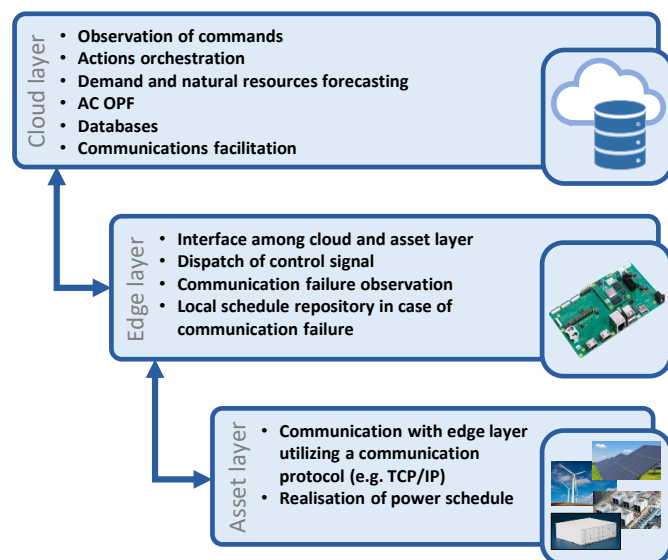
FIGURE 2. Proposed layered architecture.

This research introduces a novel three-layer architecture for multi-vector power island operation which encompasses the cloud layer, the edge layer, and the asset layer. Each layer serves a distinct but interconnected function in the overall optimization strategy.

Cloud Layer: The cloud layer is the brain of our optimization strategy, responsible for the overarching orchestration of commands and actions. It leverages advanced forecasting algorithms for demand and natural resources, performing AC OPF calculations to ensure the efficient utilization of available assets. By maintaining comprehensive databases, the cloud layer facilitates seamless communication across the network, which is vital for real-time operational agility.

Edge Layer: Serving as the intermediary, the edge layer acts as the interface between the cloud and asset layers. It ensures the reliable dispatch of control signals even in the face of communication failures, maintaining a local schedule

repository as a contingency measure. This layer's design is critical for enhancing the resilience of the power island's operation, allowing for uninterrupted control despite potential network disturbances.

Asset Layer: The asset layer is where the physical realization of the power schedule occurs. It directly communicates with the edge layer, executing the operational plans using a robust communication protocol. This layer comprises the tangible components of the power island, such as HVAC systems, batteries, and other controllable loads and resources.

The focus of this paper lies on the cloud layer, as it is the central hub for the decision-making process, integrating the flexibility and computational power of modern cloud computing to address the dynamic nature of post-islanding conditions. By prioritizing the cloud layer, we can harness the full potential of cloud-based optimization without detracting from the critical roles of the edge and asset layers, which are detailed in accordance to their supportive functions in the proposed strategy.

A detailed description of the sequence of actions pertaining to the cloud layer can be found hereafter:

1) The algorithm starts and awaits an operator request for an intentional islanding event.
2) Following a request from the operator at $t = t_0$ to prepare for an intentional islanding at $t = t_n$ (assuming t_n the intentional islanding scheme deployment), the algorithm triggers *Container 1* which is the master container with a description of the next steps. *Container 1* triggers *Container 2* and *Container 3*.
3) *Container 2* comprises the algorithm which forecasts demand, temperature, irradiance and wind speed for the next 24 hours. To facilitate that, *Container 2* utilizes a database of historical data regularly updated within a MS Azure blob storage container. It then stores the forecasted data into an output MS Azure blob storage container, which shall be later used by the AC OPF.
4) Concurrently with *Container 2*, *Container 3* initiates its processes. The first algorithm within *Container 3* checks the latest forecasting output via a *watchdog* routine every 1 second until it confirms that the forecasting routine of *Container 2* has been concluded.
5) The actual AC OPF is then initiated, gathering two types of required datasets: a) Forecasting output, and b) network topology as declared by the network operator. The AC OPF runs and produces a dataset of dispatch signals for the energy assets via the edge intelligence in order to realize it at the appropriate timing (i.e. t_n).
6) The procedure is re-initiated from Step 2 (i.e. *Container 1* triggering) to provide a new power schedule starting from t_{n+1}, where $t_{n+1} = t_n + 5$ *minutes*.

It should be noted that the AC OPF and the Forecasting modules are both constructed in a manner which provide flexibility in terms of number of assets and topological characteristics, thus rendering the solution flexible, scalable and interoperable.

IEEE *Access*

Patsidis *et al.*: Multi-Vector Power Island Operation Utilizing Demand Side Response Based on a Cloud-based Optimization Strategy (CbOS)

The forecasting container is executed upon request on the cloud. The inputs are historical data regarding demand, temperature, wind speed and irradiance. The outputs are the same variables, forecasted for the subsequent 24 hours in 5 minutes time intervals. As IoT devices gather the historical data and update the repository of each variable, Prophet tool is utilized to proceed into the 24 hour forecasting [34]. Prophet is a time series, open-source, forecasting tool developed by Facebook.

A presentation of the algorithm with its necessary building blocks, as described above, is presented in Fig. 3.
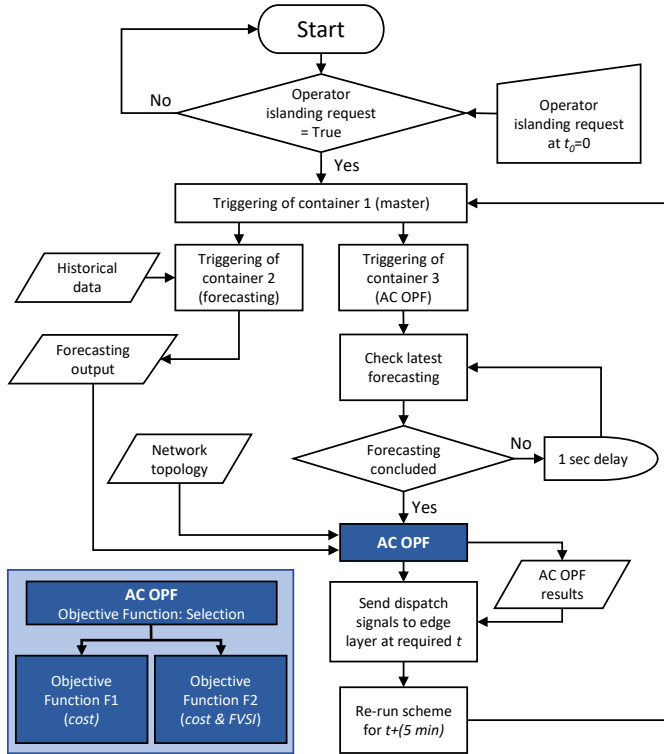

FIGURE 3. Flowchart of cloud layer operation.

B. AN AC OPF CONSIDERING DSR FROM HVAC

The AC OPF presented in this section is utilized on-demand, following a network partitioning (i.e. intentional islanding), to optimally dispatch generation, controllable and uncontrollable demand and controllable HVAC systems located within a power island in order to satisfy all operational constraints and stability limits. HVAC controllability pertains to the power regulation of the HVAC subject to satisfying the building temperature limits. It should be noted that subject to the HVAC technical characteristics, and utilizing the flexibility stemming from (21), the HVAC control can either be a thermostatic or power setting. The AC OPF presented in this section, based on the equations shown in [35], is further expanded by integrating HVAC systems and their respective mathematical formulation.

The AC OPF presented hereafter has the following unique characteristics: 1) calculates a 24 hours ahead active and

reactive power schedule in 5 minutes time intervals, thus maximizing the granularity of the dispatch and increasing the visibility to temporal variations, 2) runs every 5 minutes in a rolling window basis, guaranteeing that the latest conditions are taken into consideration few minutes prior to dispatching a control signal to an energy asset, 3) possesses feedback-based capabilities with most recent forecasting data being fed into the algorithms.

The algorithm is written in *Python* and utilizes the *Pyomo* toolbox with the *IPOPT* open-source solver to solve the non-linear AC OPF.

The objective function for the optimization problem of the power island operation is presented in (1).

$$F_1 = \min(\sum_{t \in T} \sum_{g \in N_{bus_{SG}}} Cost_{SG} \cdot (P_{SG}(g,t))$$
$$+ \sum_{t \in T} \sum_{l \in N_{bus_{LD}}} VOLL \cdot (P_{Loadshed}(l,t))) \quad (1)$$

The first term includes the operational cost of the synchronous generator and the second term is the expected cost of load shedding (assuming a static cost $Cost_{SG}$ of £200/MWh and *VOLL* cost of £3,000/MWh [36]). Aim of the optimization is to minimize the value of the objective function, as a whole (i.e., both terms with their respective weights). It is assumed that generation costs stem solely from fuel-based generating units. Note that the cost of load shedding is much higher than the cost of the synchronous generator, meaning that inherently and when applicable the AC OPF shall utilize all internal generation capabilities prior to deciding that load shedding is required.

For this study, another objective function for the AC OPF is formulated and presented in (2), which incorporates, among the cost terms presented in (1), FVSI as a third term with an accompanying weight (i.e. VOVS) in order to drive the optimization to minimize this term alike.

$$F_2 = \min(\sum_{t \in T} \sum_{g \in N_{bus_{SG}}} Cost_{SG} \cdot (P_{SG}(g,t))$$
$$+ \sum_{t \in T} \sum_{l \in N_{bus_{LD}}} VOLL \cdot (P_{Loadshed}(l,t))$$
$$+ \sum_{t \in T} \sum_{k \in N_{line_{rec}}} \sum_{v \in N_{bus_{sen}}} VOVS \cdot \frac{4 \cdot Z^2(k,t) \cdot Q_r(k,t)}{V_s^2(v,t) \cdot X(k,t)}) \quad (2)$$

The operational problem is subject to operational constraints presented by (3)-(18). (3) and (4) pertain to the active and reactive power limits of conventional synchronous generator, respectively.

$$P_{SG,min} \leq P_{SG}(g,t) \leq P_{SG,max} \ \forall t \in T, \forall g \in N_{bus_{SG}} \quad (3)$$

$$Q_{SG,min} \leq Q_{SG}(g,t) \leq Q_{SG,max} \ \forall t \in T, \forall g \in N_{bus_{SG}} \quad (4)$$

The active and reactive power limits of wind turbine generator are represented by (5) and (6), respectively.

$$0 \leq P_{WT}(g,t) \leq P_{WT,max} \ \forall t \in T, \forall g \in N_{bus_{WT}} \quad (5)$$

Patsidis *et al.*: Multi-Vector Power Island Operation Utilizing Demand Side Response Based on a Cloud-based Optimization Strategy (CbOS)

IEEE *Access*

$$0 \leq Q_{WT}(g,t) \leq Q_{WT,max} \ \forall t \in T, \forall g \in N_{bus_{WT}} \quad (6)$$

(7) and (8) correspond to the maximum active and reactive power limits of solar PV, respectively.

$$0 \leq P_{PV}(g,t) \leq P_{PV,max} \ \forall t \in T, \forall g \in N_{bus_{PV}} \quad (7)$$

$$0 \leq Q_{PV}(g,t) \leq Q_{PV,max} \ \forall t \in T, \forall g \in N_{bus_{PV}} \quad (8)$$

FVSI typically ranges from 0 to 1, with values over 1 indicating an imminent voltage collapse. In this research, CbOS utilizes either (1) or (2) to benchmark their individual performance.

Battery storage-related constraints are provided by (9) - (13). Note that (11) relates to allowing the battery to either charge or discharge at each time interval considered, while (13) guarantees that the state of charge of the battery at the end of each 24 hours horizon is the same as at the beginning of the operational cycle.

$$0 \leq S_{BESS}^c(b,t) \leq S_{BESS} \ \forall t \in T, \forall b \in N_{bus_{BESS}} \quad (9)$$

$$0 \leq S_{BESS}^d(b,t) \leq S_{BESS} \ \forall t \in T, \forall b \in N_{bus_{BESS}} \quad (10)$$

$$S_{BESS}^c(b,t) \cdot S_{BESS}^d(b,t) = 0 \ \forall t \in T, \forall b \in N_{bus_{BESS}} \quad (11)$$

$$0 \leq SoC(b,t) \leq ESTO_{max} \ \forall t \in T, \forall b \in N_{bus_{BESS}} \quad (12)$$

$$SoC(b,t) = SoC(b,t-1) +$$
$$(\eta_c \cdot S_{BESS}^c(b,t) - \eta_d \cdot S_{BESS}^d(b,t)) \cdot \Delta t,$$
$$\forall t \in T - \{1\}, \forall b \in N_{bus_{BESS}} \quad (13)$$

The active and reactive power balance equations at each bus b are represented by (14) and (15), respectively, where $P_b^{ex}(t)$ and $Q_b^{ex}(t)$ are given by (16) and (17), which are the classical equations pertaining to power flow problems.

$$S_{BESS}^d(b,t) - S_{BESS}^c(b,t) + \sum_{g \in N_{bus}} P(g,t) + P_{Loadshed}(b,t)$$
$$= P^{ex}(b,t) + P_{LD}(b,t) + K_{HVAC}(b,t) \cdot S_{HVAC} \quad (14)$$

$$\sum_{g \in N_{bus}} Q(g,t) + Q_{Loadshed}(b,t)$$
$$= Q^{ex}(b,t) + Q_{LD}(b,t) \quad (15)$$

$$P^{ex}(b,t) = \sum_{p \in N_{br}} V(b,t) \cdot V(p,t) \cdot (G_{bp} \cdot cos\delta_{bp}(t) +$$
$$B_{bp} \cdot sin\delta_{bp}(t)) \ \forall t \in T, \forall b \in N_{br} \quad (16)$$

$$Q^{ex}(b,t) = \sum_{p \in N_{br}} V(b,t) \cdot V(p,t) \cdot (G_{bp} \cdot sin\delta_{bp}(t) -$$
$$B_{bp} \cdot cos\delta_{bp}(t) \ \forall t \in T, \forall b \in N_{br} \quad (17)$$

(18) corresponds to the limit of available load shedding at each time.

$$P_{Loadshed}(l,t) \leq P_{LD}(l,t) \ \forall t \in T, \forall l \in N_{bus_{LD}} \quad (18)$$

Finally, (19) and (20) represent voltage and line capacity constraints, respectively.

$$V_{min} \leq V(v,t) \leq V_{max} \ \forall t \in T, \forall v \in N_{bus} \quad (19)$$

$$max(S(i,t)) \leq S_{max}^i \ \forall t \in T, \forall i \in N_{br} \quad (20)$$

To integrate HVAC within the optimal power flow formulation, the thermodynamic equation represented by (21) and proposed in [20] was formulated. This equation describes the temperature within a building with specific thermal characteristics and an installed HVAC system. The constraints accompanying the HVAC operation are represented by (22) and (23).

$$T_{bld}(b,t+1) = T_{ambient}(b,t+1) + H \cdot R_{TH} \cdot K_{HVAC}(b,t) -$$
$$(T_{ambient}(b,t+1) + H \cdot R_{TH} \cdot K_{HVAC}(b,t) - T_{bld}(b,t))e^{\Delta t/RC}$$
$$\forall t \in T - \{1\}, \forall b \in N_{bus_{HVAC}} \quad (21)$$

$$0 \leq K_{HVAC}(b,t) \leq 1, \forall t \in T, \forall b \in N_{bus_{HVAC}} \quad (22)$$

$$T_{bld,min} \leq T_{bld}(b,t) \leq T_{bld,max}$$
$$\forall t \in T, \forall b \in N_{bus_{HVAC}} \quad (23)$$

The implementation of our AC OPF model leverages the hidden flexibility of HVAC systems—this flexibility allows for adjustments in energy use by HVAC systems that maintain comfort levels within acceptable ranges while contributing to demand-side management. Specifically, we demonstrate how this flexibility can be utilized to mitigate the need for load shedding by providing additional demand-side responsiveness. This responsiveness is crucial in maintaining grid stability, especially in scenarios where renewable generation may not fully meet demand.

The hidden flexibility of HVAC systems is harnessed through dynamic adjustments in their operation, including but not limited to, modulation of temperature setpoints. These adjustments allow HVAC systems to contribute to grid stability in an active manner.

III. DESCRIPTION OF CASE STUDIES

Two main scenarios with representative case studies have been conducted as part of this research, with respect to the level and extent of controllability that the operator possesses over various assets. Each category is then investigated with respect to the utilization of either objective function (1) or (2) and results were drawn for different HVAC comfort limits. Assuming that the initial intentional islanding scheme deployed created an imbalance between the local load and generation, the following operational scenarios are explored to restore the power balance before moving into an unstable locus of operation:

IEEE *Access*

Patsidis *et al.*: Multi-Vector Power Island Operation Utilizing Demand Side Response Based on a Cloud-based Optimization Strategy (CbOS)

1) Scenario I: Local generation $\leq$ local demand, with the cloud-hosted architecture having controllability solely over demand and HVAC.
2) Scenario II: Local generation $\leq$ local demand, with the cloud-hosted architecture having controllability over all energy assets.

For each of the scenarios described above, the following cases were explored, thus creating a set of four different arrangements (i.e. I.a., I.b., II.a., II.b.):

- Case a: Objective function described by (1) (i.e. only cost is considered) and HVAC comfort limit set at $20°C$, $19°C$, $18°C$ and $17°C$.
- Case b: Objective function described by (2) (i.e. cost and voltage stability index are both considered) and HVAC comfort limit set at $20°C$, $19°C$, $18°C$ and $17°C$.

The detailed description of the problem, as formulated in the previous sections, has been applied to a 7-bus meshed distribution network presented in Fig. 4.
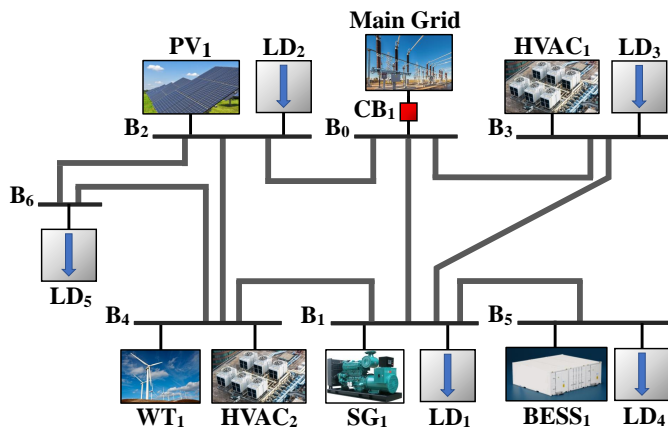

FIGURE 4. Case study 7-bus power island.

In this paper, the selection of a 7-bus meshed distribution network as our primary model for simulation and analysis was driven by strategic considerations. This model size strikes an optimal balance between complexity and clarity, allowing for the nuanced demonstration of the proposed CbOS capabilities. The 7-bus network, while compact, encapsulates the energy asset classes and challenges of larger power systems, making it an ideal test-bed for innovative strategies like CbOS. Its use facilitates a focused investigation into the effectiveness of integrating HVAC flexibility for voltage stability improvements, without the computational, analytical and cloud cost overheads associated with larger scale systems. Importantly, the chosen network enables a detailed, step-by-step illustration of CbOS's impact on operational efficiency and cost reduction, ensuring that the advantages of our approach are comprehensively communicated.

The post-contingency islanded network comprises technologies that are already integrated into power systems, including Synchronous Generator (SG), Solar Photovoltaic (PV), Wind Turbine (WT), Battery Energy Storage System (BESS), load (LD) and HVAC. The PV capacity is set at 50 kW, WT at 100 kW, SG at 200 kW, BESS at 200 kW/300 kWh while the HVAC systems, which are assumed to be installed at industrial and/or commercial facilities are rated at 200 kW each. It should be noted that we assume the presence of grid-forming capability within the power island. The algorithm which decides the optimal network partitioning shall include this within the problem formulation. The building thermal parameters H, R_{TH} and C, as proposed in [20], are set to 400 W, $0.121 °C/W$ and $3599 J/°C$, respectively, and considered the same for all HVAC-served premises. The line parameters of the test network are presented in Table 1 (the per-unit values corresponding to a base value of 1 MVA at 11 kV).

TABLE 1. Network Parameters

Line	From Bus	To Bus	R (p.u.)	X (p.u.)
L_{01}	0	1	0.0611	0.0079
L_{02}	0	2	0.1222	0.0158
L_{03}	0	3	0.0815	0.0105
L_{13}	1	3	0.0764	0.0099
L_{14}	1	4	0.1528	0.0198
L_{15}	1	5	0.1834	0.0238
L_{24}	2	4	0.1019	0.0132
L_{26}	2	6	0.1834	0.0198
L_{46}	4	6	0.1528	0.0148

Commencing at t_n, CB_1 opens and concurrently the network is operated by the cloud-hosted optimization system. It is assumed that prior to the disconnection with the main grid, the power island was a net power importer. For the results depicted in the subsequent cases, we assume that $t_n=0$.

A. SCENARIO I - NETWORK OPERATION WITH LIMITED ENERGY ASSETS CONTROLLABILITY

In Scenario I, the optimization algorithm is tuned to operate and control solely the demand (i.e. load shedding and controllable load) and HVAC systems. In that case, the generating assets (i.e. SG, WT, PV and BESS) are operating according to a mix of maximum available resources and/or pre-contingency schedules. The schedule is used as an input, instead of a set of variables, for the AC OPF. The forecasting algorithm, considering a historical set of wind speed, solar irradiance, demand, and temperature generated a forecast for the parameters which are illustrated in Fig. 5.

A typical schedule which was used for Scenario I is presented in Fig. 6, with 1) renewable generation operating under maximum power point tracking (MPPT) and thus producing the maximum available power, subject to the natural resource availability, 2) BESS operating under a pre-defined schedule and 3) SG (not depicted) operating at 180 kW throughout the 24 hours duration.

1) Case a - Objective function to minimize cost introduced by SG and load shedding

In the baseline scenario, the HVAC has a setting of $T_{bld,min} =20.9°C$ and an initial T_{bld} of $21°C$. Then the same operating scenario is run with $T_{bld,min}$ set at $20°C$, $19°C$,
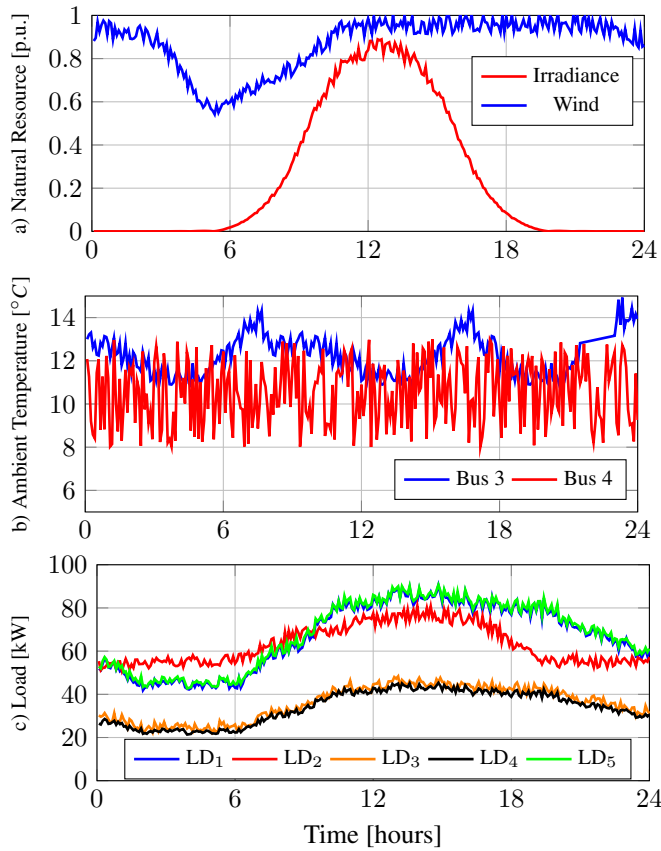
This article has been accepted for publication in IEEE Access. This is the author's version which has not been fully edited and content may change prior to final publication. Citation information: DOI 10.1109/ACCESS.2024.3384985

Patsidis *et al.*: Multi-Vector Power Island Operation Utilizing Demand Side Response Based on a Cloud-based Optimization Strategy (CbOS)

IEEE *Access*

FIGURE 5. Natural resources (wind, irradiance) and load forecast.
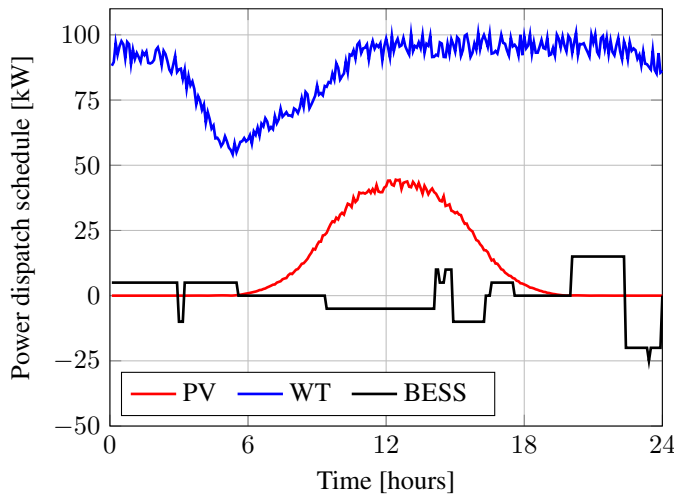
FIGURE 6. Power schedule for cases of Scenario I.

$18°C$ and finally $17°C$ which is assumed to be the lowest temperature which does not significantly affect the occupants comfort. Please note that HVAC systems can be found in both domestic (e.g. family homes) and commercial (e.g. industrial plants, office buildings, etc.) deployments.

For each of these $T_{bld,min}$ settings, the AC OPF calculates

the necessary load shedding required to maintain the sustainability of the power island, with the objective function examined being (1). The results are presented in Fig. 7(a). The results show that as the $T_{bld,min}$ and thus the required power from HVAC systems is decreased, the island requires less load shedding to reach a power equilibrium.
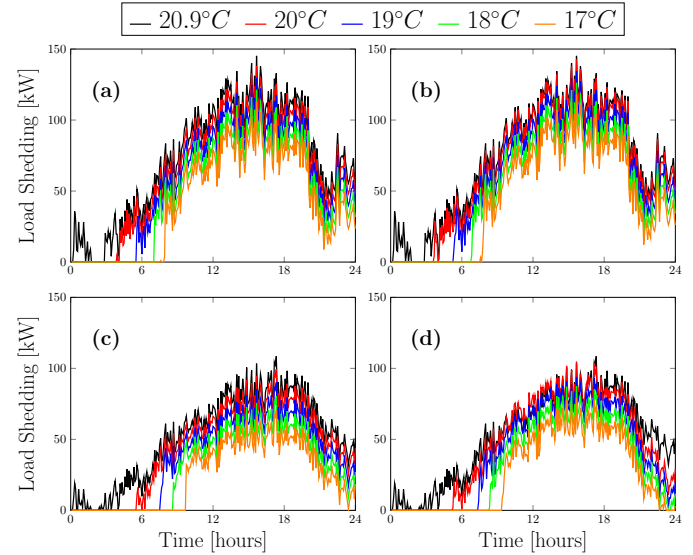

FIGURE 7. Load shedding required for Scenario I.a. (a), I.b. (b), II.a (c). and II.b. (d).

The voltage stability index FVSI of each line is also calculated for this set of results and illustrated in Fig. 8(a). L_{46} sporadically exhibits values over 1.0 (i.e. stability limit) which indicates that the line is over the stability limit and close to voltage instability and collapse. Note that only the results for the baseline scenario of $T_{bld,min}$ set at $20.9°C$ are presented as no significant differences (i.e. ≤ 0.001) in FVSI indices were observed in other $T_{bld,min}$ settings.

2) Case b: Objective function to minimize cost introduced by SG and load shedding and FVSI

To mitigate this issue and investigate the additional value of considering voltage stability as part of the objective function, the same problem was reformulated and run, with the objective this time being mathematically formulated by (2).

The load shedding required to operate the island in balanced conditions is shown in Fig. 7(b). For $T_{bld,min}$ settings of $20°C$, $19°C$, $18°C$ and $17°C$ there is a slight increase in load shedding, namely 5%, 5.5%, 6.1% and 7% increase in overall shedding, however there is concurrently a significant improvement of the FVSI indices, especially at L_{46} from 1.05 to 0.96, i.e. a 8.57% FVSI decrease which sets the line below the stability limit of 1.0. The FVSI of all lines for Scenario I.b. are presented in Fig. 8(b).

A comparison among the maximum values of FVSI for each line, with both objective functions (i.e. (1) and (2)) under Scenario I is depicted in Fig. 9. Without the provision of the solution proposed in this paper, the power island faces two
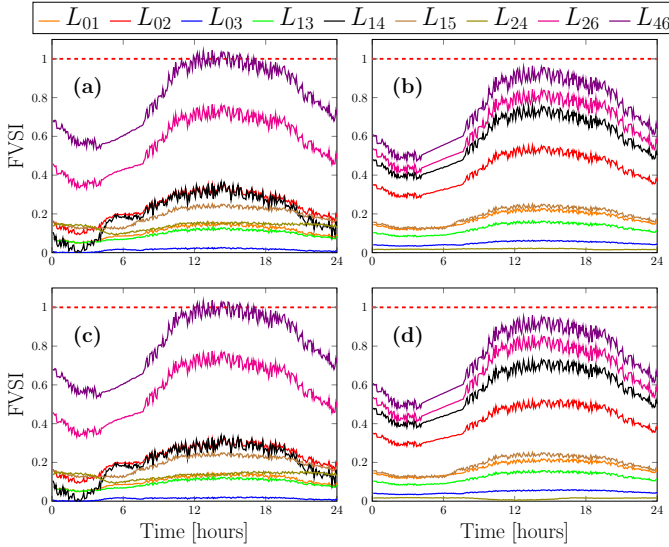
FIGURE 8. 24-hour FVSI profiles of all lines for Scenarios I.a. (a), I.b. (b), II.a (c). and II.b. (d).

main challenges: 1) Technically, the voltage will collapse due to FVSI values exceeding the safe region, and 2) financially, the cost of operating it will be substantially more due to the required load shedding.

B. SCENARIO II - NETWORK OPERATION WITH CONTROLLABILITY OVER ALL ENERGY ASSETS

This work further investigates the added value introduced when the optimization-based control is further expanded in controlling both power consuming and generating assets. To demonstrate the impact of controllability over all energy assets, the overall architecture was altered to facilitate the additional generating units, namely SG, PV, WT and BESS.

To maintain uniformity between Scenario I and II, the forecasting module was fed with the same historical databases (i.e. no additional updates on databases) and regressors (i.e. initialization instant) in order to force the generation of the same forecast for the natural resources, demand and temperatures depicted in Fig. 5.

The overall system is triggered and following generation of the required forecasting, the AC OPF proceeds into solving the optimization problem subject to network and assets constraints discussed in Section 2. The evaluated scenarios were again evaluated under two testing variables 1) objective function and 2) HVAC comfort level. A baseline scenario was utilized to serve as a benchmark in which the HVAC is again set with a $T_{bld,min}$ thermostat setting of $20.9°C$ and an initial T_{bld} of $21°C$. Identically with Scenario I, the baseline case is repeated under $T_{bld,min}$ thermostat settings of $20°C$, $19°C$, $18°C$ and $17°C$ for both objective functions described in (1) and (2).

1) Case a: Objective function to minimize cost introduced by SG and load shedding

For each of these $T_{bld,min}$ settings, the AC OPF calculates the necessary power setpoint of the generating assets, load shedding required to maintain the sustainability of the power island, with the objective function utilized being (1). Even though there is controllability over the generating assets, the available capacity and natural resources are not sufficient to cover the local demand. Consequently, the AC OPF proceeds into shedding the necessary load to maintain the balance within the power island. The load shedding required for each $T_{bld,min}$ setting is presented in Fig. 7(c). Note that the additional controllability over the generating assets, allows the power island to operate with lower load shedding, with respect to the load shedding required for both cases of Scenario I. The voltage stability index FVSI is also illustrated in Fig. 8(c), with the FVSI index of L_{46} reaching values of over 1.0 under high system stress, rendering the line prone to voltage collapse.

Similarly to Scenario I, note that solely the FVSI results from the $T_{bld,min} = 20.9°C$ are shown, as no significant deviations (i.e. ≤ 0.001) were observed in other $T_{bld,min}$ cases of this scenario.

2) Case b: Objective function to minimize cost introduced by SG and load shedding and FVSI

Even though the load shedding is significantly affected by the integration of control on the generating assets, FVSI index of L_{46} is still at a critical value of 1.04, 4% above the stability limit. To alleviate the issue, this subsection focuses on examining the utilization of objective function defined by (2), thus considering additionally considering the voltage stability index FVSI of all lines of the network part of the objective function.

Again, the network operation was investigated under $T_{bld,min}$ settings of $20°C$, $19°C$, $18°C$ and $17°C$. The load shedding required to balance the network for each $T_{bld,min}$ is presented in Fig. 7(d). It is observed that there is an increase in total load shedding required for each case of Scenario II.b. where voltage stability is part of the objective function, namely 6.8% for $T_{bld,min} = 20°C$, 7.7% for $T_{bld,min} = 19°C$, 9.1% for $T_{bld,min} = 18°C$ and 11% for $T_{bld,min} = 17°C$ with respect to the results obtained for Scenario II.a.

Nevertheless, the slight increase of total load shedding required is accompanied by an improvement of FVSI indices, as demonstrated in Fig. 8(d). Specifically, FVSI index of line L_{46}, which would be subject to voltage collapse when optimizing only the operational cost, has a value of 0.95, a 8.7% decrease from its previous value of 1.04, thus rendering the line voltage-stable according to FVSI stability limit of 1.0.

A comparison between the maximum observed FVSI values for each network branch with respect to the objective function utilized under Scenario II is illustrated in Fig. 9. Again, it is evident that the optimisation of FVSI helps reduce the stress of branch L_{46}.
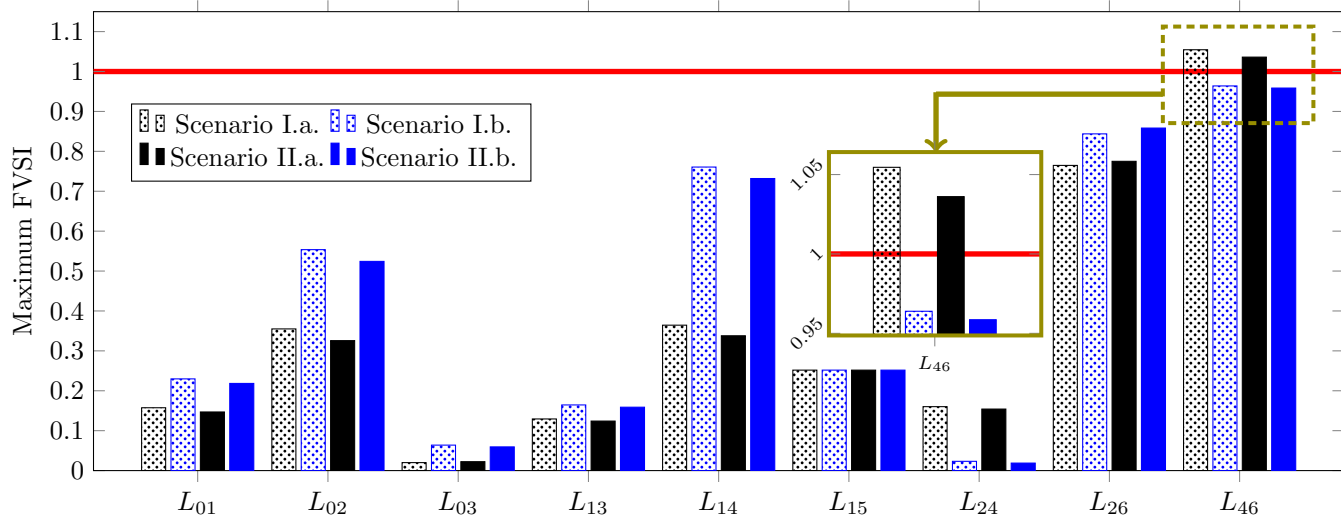
Patsidis *et al.*: Multi-Vector Power Island Operation Utilizing Demand Side Response Based on a Cloud-based Optimization Strategy (CbOS)

IEEE *Access*

FIGURE 9. Maximum FVSI of all lines for Scenarios I.a., I.b., II.a. and II.b.

C. DISCUSSION

While Figures 7 and 8 might initially suggest similarities across scenarios, a closer examination of the quantitative outcomes reveals substantial differences. For instance, the reduction in load shedding achieved by leveraging HVAC flexibility—though visually subtle between Fig. 7(a) and 7(c)—is quantitatively significant and in the region of 25%.

Similarly, the improvements in voltage stability metric FVSI, as depicted in Fig. 8, is notable. Lines with FVSI over 1.00 are considered voltage unstable. The results presented in Fig. 8, and specifically the FVSI reduction shown in Fig. 8(b) and Fig. 8(d) highlight the efficacy of the cloud-based optimization strategy (CbOS) in enhancing microgrid resilience and increased voltage stability.

The remainder of this section serves as a cost-level comparison among the case studies presented above. Fig. 10 illustrates the cost comparison of operating the power island under both cases of Scenario I and II, with various $T_{bld,min}$ settings.

The quantitative results show that extending the deployment of the method to generating assets and not solely demand and HVAC yields a cost reduction spanning from 22.2%-31% for same $T_{bld,min}$ settings. Similar results are observed in Fig 10, where (2) was used as objective function. In that case, Scenario II costs were reduced by 23.7%-29.9% for same $T_{bld,min}$ settings.

The second additional benefit, stemming from adjusting the $T_{bld,min}$ setting to lower comfort levels is also evident: Reducing the comfort levels from the default $20.9°C$ to $17°C$ while controlling both demand and generation results into a 55.6% cost reduction when using objective function (1). The corresponding metric when (2) was used as objective function is 49.6%. In terms of optimizing both cost and voltage stability, among case studies with the same $T_{bld,min}$ setting, a cost increase of 4.2%-7.1% was observed which shall be taken into
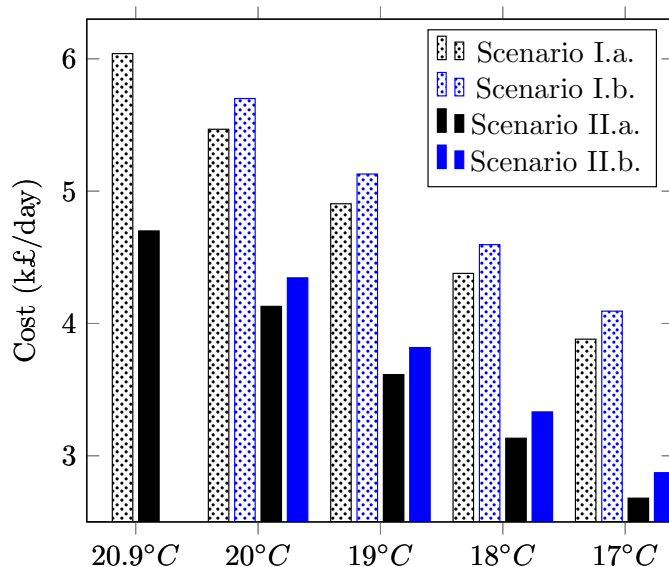

FIGURE 10. Cost comparison for Scenario I.a., I.b., II.a. and II.b.

consideration under a cost-benefit analysis (CBA), however the authors believe that the impact of a voltage collapse under emergency conditions justifies the additional cost.

IV. CONCLUSIONS

This paper addresses fundamental challenges pertaining to 1) the operation of a contingency-triggered multi-vector power island with minimum consumers disruption and better stability profiles and 2) providing system operators with flexible and scalable tools that can be used during contingencies. Both challenges are addressed by the CbOS proposed in this paper. It has been demonstrated that the deployment of a cloud-hosted, contingency-triggered, optimization-based control scheme is possible at a low cost (considering the low

IEEE *Access*

Patsidis *et al.*: Multi-Vector Power Island Operation Utilizing Demand Side Response Based on a Cloud-based Optimization Strategy (CbOS)

cost of maintaining an active container repository and edge devices), thus rendering the solution desirable for network operators which would otherwise not necessarily invest at a low-probability contingency.

First, we propose a strategy which bridges the gap between the multi-vector energy assets and the system operator through a multi-layered approach. At the core of the proposition, CbOS receives the operator commands and proceeds into orchestrating the actions necessary to optimize and operate the power island. Then we devise the problem in the form of an AC OPF and we unlock the HVAC flexibility potential by formulating and integrating it into the AC OPF, hosted within CbOS. Furthermore, we incorporate an additional term to optimize both cost and voltage stability, in order to maintain the sustainability of the power island and alleviate the risk of voltage collapse. To validate our proposition, the strategy is benchmarked under representative case studies, with respect to the extent of controllability that CbOS possesses. Simulation results indicate that the CbOS can effectively optimize the voltage stability when required, with results showing a voltage stability index improvement up to 8.7% for lines under stress, while comparatively reducing the operational cost up to 55.6% by harnessing the hidden flexibility of HVAC.

REFERENCES

[1] Y. Sha, W. Li, J. Yan, W. Li, and X. Huang, "Research on investment scale calculation and accurate management of power grid projects based on three-level strategy," *IEEE Access*, vol. 9, pp. 67 176–67 185, 2021.

[2] L. C. da Costa, F. S. Thomé, J. D. Garcia, and M. V. F. Pereira, "Reliability-constrained power system expansion planning: A stochastic risk-averse optimization approach," *IEEE Transactions on Power Systems*, vol. 36, no. 1, pp. 97–106, 2021.

[3] G. A. Nakas and P. N. Papadopoulos, "Investigation of cascading events in power systems with renewable generation," in *2020 IEEE PES Innovative Smart Grid Technologies Europe (ISGT-Europe)*, 2020, pp. 211–216.

[4] A. Mishra and P. Jena, "A scheduled intentional islanding method based on ranking of possible islanding zone," *IEEE Transactions on Smart Grid*, vol. 12, no. 3, pp. 1853–1866, 2021.

[5] P. Demetriou, J. Quirós-Tortós, and E. Kyriakides, "When to island for blackout prevention," *IEEE Systems Journal*, vol. 13, no. 3, pp. 3326–3336, 2019.

[6] P. Demetriou, M. Asprou, and E. Kyriakides, "A real-time controlled islanding and restoration scheme based on estimated states," *IEEE Transactions on Power Systems*, vol. 34, no. 1, pp. 606–615, 2019.

[7] A. Kyriacou, P. Demetriou, C. Panayiotou, and E. Kyriakides, "Controlled islanding solution for large-scale power systems," *IEEE Transactions on Power Systems*, vol. 33, no. 2, pp. 1591–1602, 2018.

[8] J. Xu, B. Xie, S. Liao, Z. Yuan, D. Ke, Y. Sun, X. Li, and X. Peng, "Load shedding and restoration for intentional island with renewable distributed generation," *Journal of Modern Power Systems and Clean Energy*, vol. 9, no. 3, pp. 612–624, 2021.

[9] J. R. Monteiro, Y. R. Rodrigues, M. R. Monteiro, A. C. Z. De Souza, and B. I. L. Fuly, "Intelligent rmps allocation for microgrids support during scheduled islanded operation," *IEEE Access*, vol. 8, pp. 117 946–117 960, 2020.

[10] S. Wen, S. Wang, G. Liu, and R. Liu, "Energy management and coordinated control strategy of pv/hess ac microgrid during islanded operation," *IEEE Access*, vol. 7, pp. 4432–4441, 2019.

[11] S. Negri, E. Tironi, and D. S. Danna, "Integrated control strategy for islanded operation in smart grids: Virtual inertia and ancillary services," *IEEE Transactions on Industry Applications*, vol. 55, no. 3, pp. 2401–2411, 2019.

[12] P. P. Vergara, J. M. Rey, J. C. López, M. J. Rider, L. C. da Silva, H. R. Shaker, and B. N. Jørgensen, "A generalized model for the optimal operation of microgrids in grid-connected and islanded droop-based mode," *IEEE Transactions on Smart Grid*, vol. 10, no. 5, pp. 5032–5045, 2019.

[13] M. Dabbaghjamanesh, B. Wang, A. Kavousi-Fard, S. Mehraeen, N. D. Hatziargyriou, D. N. Trakas, and F. Ferdowsi, "A novel two-stage multi-layer constrained spectral clustering strategy for intentional islanding of power grids," *IEEE Transactions on Power Delivery*, vol. 35, no. 2, pp. 560–570, 2020.

[14] M. R. Aghamohammadi, S. F. Mahdavizadeh, and Z. Rafiee, "Controlled islanding based on the coherency of generators and minimum electrical distance," *IEEE Access*, vol. 9, pp. 146 830–146 840, 2021.

[15] G. Tian, S. Faddel, Q. Zhou, Z. Qu, and A. Parlato, "Optimal coordination of hvac scheduling for commercial buildings," in *2020 IEEE Texas Power and Energy Conference (TPEC)*, 2020, pp. 1–5.

[16] B. Tashtoush, M. Molhim, and M. A. Al-Rousan, "Dynamic model of an hvac system for control analysis," *Energy*, vol. 30, pp. 1729–1745, 2005.

[17] A. Thosar, A. Patra, and S. Bhattacharyya, "Feedback linearization based control of a variable air volume air conditioning system for cooling applications," *ISA transactions*, vol. 47 3, pp. 339–49, 2008.

[18] C. Diakaki, E. Grigoroudis, and D. Kolokotsa, "Towards a multi-objective optimization approach for improving energy efficiency in buildings," *Energy and Buildings*, vol. 40, pp. 1747–1754, 2008.

[19] B. Wang, Y. Li, W. Ming, and S. Wang, "Deep reinforcement learning method for demand response management of interruptible load," *IEEE Transactions on Smart Grid*, vol. 11, no. 4, pp. 3146–3155, 2020.

[20] N. Lu and Y. Zhang, "Design considerations of a centralized load controller using thermostatically controlled appliances for continuous regulation reserves," *IEEE Transactions on Smart Grid*, vol. 4, no. 2, pp. 914–921, 2013.

[21] D. Muthirayan, D. Kalathil, K. Poolla, and P. Varaiya, "Mechanism design for demand response programs," *IEEE Transactions on Smart Grid*, vol. 11, no. 1, pp. 61–73, 2020.

[22] D. S. Markovic, D. Zivkovic, I. Branovic, R. Popovic, and D. Cvetkovic, "Smart power grid and cloud computing," *Renewable and Sustainable Energy Reviews*, vol. 24, pp. 566–577, 2013.

[23] K. Kaur, T. Dhand, N. Kumar, and S. Zeadally, "Container-as-a-service at the edge: Trade-off between energy efficiency and service availability at fog nano data centers," *IEEE Wireless Communications*, vol. 24, no. 3, pp. 48–56, 2017.

[24] C. Pahl, A. Brogi, J. Soldani, and P. Jamshidi, "Cloud container technologies: A state-of-the-art review," *IEEE Transactions on Cloud Computing*, vol. 7, no. 3, pp. 677–692, 2019.

[25] S. Zhang, A. Pandey, X. Luo, M. Powell, R. Banerji, L. Fan, A. Parchure, and E. Luzcando, "Practical adoption of cloud computing in power systems—drivers, challenges, guidance, and real-world use cases," *IEEE Transactions on Smart Grid*, vol. 13, no. 3, pp. 2390–2411, 2022.

[26] A. Bachoumis, N. Andriopoulos, K. Plakas, A. Magklaras, P. Alefragis, G. Goulas, A. Birbas, and A. Papalexopoulos, "Cloud-edge interoperability for demand response-enabled fast frequency response service provision," *IEEE Transactions on Cloud Computing*, vol. 10, no. 1, pp. 123–133, 2022.

[27] Y. Tao, J. Qiu, and S. Lai, "A hybrid cloud and edge control strategy for demand responses using deep reinforcement learning and transfer learning," *IEEE Transactions on Cloud Computing*, vol. 10, no. 1, pp. 56–71, 2022.

[28] H.-M. Chung, S. Maharjan, Y. Zhang, F. Eliassen, and K. Strunz, "Optimal energy trading with demand responses in cloud computing enabled virtual power plant in smart grids," *IEEE Transactions on Cloud Computing*, vol. 10, no. 1, pp. 17–30, 2022.

[29] D. Sehloff, M. Marathe, A. Manur, and G. Venkataramanan, "Self-sufficient participation in cloud-based demand response," *IEEE Transactions on Cloud Computing*, vol. 10, no. 1, pp. 4–16, 2022.

[30] M. A. Jirjees, D. A. Al-Nimma, and M. S. M. Al-Hafidh, "Selection of proper voltage stability index for real system loading," in *2019 2nd International Conference on Electrical, Communication, Computer, Power and Control Engineering (ICECCPCE)*, 2019, pp. 62–67.

[31] A. Chandra, A. K. Pradhan, and A. K. Sinha, "A comparative study of voltage stability indices used for power system operation," in *2016 21st Century Energy Needs - Materials, Systems and Applications (ICTFCEN)*, 2016, pp. 1–4.

[32] A. Alshareef, R. Shah, N. Mithulananthan, and S. Alzahrani, "A new global index for short term voltage stability assessment," *IEEE Access*, vol. 9, pp. 36 114–36 124, 2021.

[33] I. Musirin and T. Rahman, "On-line voltage stability based contingency ranking using fast voltage stability index (fvsi)," in *IEEE/PES Transmission and Distribution Conference and Exhibition*, vol. 2, 2002, pp. 1118–1123 vol.2.

[34] S. J. Taylor and B. Letham, "Forecasting at scale," *PeerJ Preprints*, 2017.

IEEE *Access*

[35] A. O. Rousis, I. Konstantelos, and G. Strbac, "A planning model for a hybrid ac–dc microgrid using a novel ga/ac opf algorithm," *IEEE Transactions on Power Systems*, vol. 35, no. 1, pp. 227–237, 2020.

[36] E. Bucaj, "278/10 - value of lost load review process," London, United Kingdom, Tech. Rep., 2018.

DIMITRIOS TZELEPIS (Member, IEEE) serves as a Visiting Lecturer at the University of Strathclyde and holds the positions of CTO and Co-Founder at SMPnet. Motivated by a foundational passion for grid digitalization, he is dedicated to developing intelligent solutions that ensure the secure, reliable, and fully-automated operation of software-defined electricity grids. Tzelepis has led the way in both research and commercial projects, created patented solutions for the power sector, and has been instrumental in formulating and revising grid codes for the UK, Europe, and Asia. His research domains encompass power system control, protection, and automation, with a special focus on integrating renewable energy sources and high-voltage direct current interconnections. His extensive experience includes profound knowledge in the integration of international standards and protocols for the development of grid control systems. He plays strategic roles in various technical committees aimed at decarbonizing the energy sector, including engagements with CIGRE, the Global Smart Grids Innovation Hub in Spain, and several Research and Development Committees working to draft and refine Grid Codes.

•••

ANGELOS PATSIDIS (Student Member, IEEE) received the M.Eng. degree in Electrical and Computer Engineering from the Democritus University of Thrace, Greece, in 2017, and the M.Sc. degree in Wind Energy Systems from the University of Strathclyde, Glasgow, U.K., in 2018, where he is currently pursuing the Ph.D. degree with the Department of Electronic and Electrical Engineering. His main research interests include power systems operation, management, optimization, control, automation, utilization of cloud computing in energy systems, and integration of distributed generation. His main research methods include implementation of intelligent algorithms and digital architecture for optimisation, real-time control, monitoring and analytics.

ADAM DYŚKO (Member, IEEE) received the Ph.D. degree in Electrical and Electronic Engineering from the University of Strathclyde, Glasgow, Scotland, in 1998. He is currently a Reader with the Department of Electronic and Electrical Engineering. He teaches a variety of Electrical Engineering subjects and has been leading several research projects with both academic and industrial partners. His research interests include power system protection, control and stability, and power quality.

CAMPBELL D. BOOTH (Senior Member, IEEE) received the B.Eng. and Ph.D. degrees in electrical and electronic engineering from the University of Strathclyde, Glasgow, Scotland, in 1991 and 1996, respectively. He is currently a Professor and presently serving as Vice Dean - Research, in the Faculty of Engineering, having previously held the position of Head of the EEE Department from 2017-2021, at the University of Strathclyde, Glasgow, U.K. His research interests include power system protection; plant condition monitoring and intelligent asset management; applications of intelligent system techniques to power system monitoring, protection, and control, knowledge management, and decision.